

# Metadata of the article that will be visualized in OnlineFirst

ArticleTitle	Sub-rectangular Tunnel Behaviour under Static Loading	
Article Sub-Title		
Article CopyRight	The Author(s), under exclusive licence to Springer Science+Business Media, LLC, part of Springer Nature (This will be the copyright line in the final PDF)	
Journal Name	Transportation Infrastructure Geotechnology	
Corresponding Author	FamilyName	<b>Dias</b>
	Particle	
	Given Name	<b>Daniel</b>
	Suffix	
	Division	Laboratory 3SR
	Organization	CNRS UMR 5521, Grenoble Alpes University
	Address	38000, Grenoble, France
	Phone	
	Fax	
	Email	daniel.dias@3sr-grenoble.fr
	URL	
	ORCID	<a href="http://orcid.org/0000-0003-2238-7827">http://orcid.org/0000-0003-2238-7827</a>
Author	FamilyName	<b>Pham</b>
	Particle	
	Given Name	<b>Van Vi</b>
	Suffix	
	Division	Faculty of Civil Engineering
	Organization	Hanoi University of Mining and Geology
	Address	Bắc Từ Liêm, Vietnam
	Phone	
	Fax	
	Email	
	URL	
	ORCID	<a href="http://orcid.org/0000-0001-9586-0406">http://orcid.org/0000-0001-9586-0406</a>
Author	FamilyName	<b>Do</b>
	Particle	
	Given Name	<b>Ngoc Anh</b>
	Suffix	
	Division	Department of Underground and Mining Construction, Faculty of Civil Engineering
	Organization	Hanoi University of Mining and Geology
	Address	Bắc Từ Liêm, Vietnam
	Phone	
	Fax	
	Email	
	URL	
	ORCID	<a href="http://orcid.org/0000-0002-4862-1688">http://orcid.org/0000-0002-4862-1688</a>
Author	FamilyName	<b>Nguyen</b>
	Particle	
	Given Name	<b>Chi Thanh</b>
	Suffix	

Division Faculty of Civil Engineering  
Organization Hanoi University of Mining and Geology  
Address Bắc Từ Liêm, Vietnam  
Phone  
Fax  
Email  
URL  
ORCID

---

Author	FamilyName	<b>Dang</b>
	Particle	
	Given Name	<b>Van Kien</b>
	Suffix	
	Division	Faculty of Civil Engineering
	Organization	Hanoi University of Mining and Geology
	Address	Bắc Từ Liêm, Vietnam
	Phone	
	Fax	
	Email	
	URL	
	ORCID	<a href="http://orcid.org/0000-0001-8821-9178">http://orcid.org/0000-0001-8821-9178</a>

---

Schedule	Received	
	Revised	
	Accepted	5 Feb 2022

---

**Abstract** Circular- and rectangular-shaped tunnels are usually utilized when excavating at shallow depths in urban areas. Nevertheless, special-shaped tunnels such as sub-rectangular tunnels were recently considered to be used for overcoming some drawbacks of circular and rectangular tunnels in terms of low utilization space ratio and stress concentration at the corners, respectively. Using numerical analyses, this paper focuses on indicating the different behaviour of sub-rectangular tunnels under static loading in comparison with circular and rectangular ones having the same utilization space. It allows designers to decide the appropriate tunnel shape solution that should be used. The influence of parameters, including soil deformability, lateral earth pressure coefficient, and lining thickness, on the behaviour of different tunnel shapes under static loadings is also investigated. The results indicated a significant difference in the behaviour of sub-rectangular tunnels in comparison with the circular and rectangular ones when considering no-slip and full-slip conditions for the soil–lining interaction.

---

**Keywords (separated by '-')** Sub-rectangular tunnel - Static load - Tunnel lining - Numerical analysis

---

**Footnote Information** - Behaviour of differently shaped tunnel linings subjected to static loading was highlighted;- Sub-rectangular tunnels can be an effective solution replacing circular and rectangular tunnel.

---



## 2 Sub-rectangular Tunnel Behaviour under Static Loading

3 Van Vi Pham<sup>1</sup> · Ngoc Anh Do<sup>2</sup> · Daniel Dias<sup>3</sup> · Chi Thanh Nguyen<sup>1</sup> ·  
4 Van Kien Dang<sup>1</sup>

5 Accepted: 5 February 2022

6 © The Author(s), under exclusive licence to Springer Science+Business Media, LLC, part of Springer Nature  
2022

### 7 Abstract

8 Circular- and rectangular-shaped tunnels are usually utilized when excavating at  
9 shallow depths in urban areas. Nevertheless, special-shaped tunnels such as sub-  
10 rectangular tunnels were recently considered to be used for overcoming some draw-  
11 backs of circular and rectangular tunnels in terms of low utilization space ratio and  
12 stress concentration at the corners, respectively. Using numerical analyses, this  
13 paper focuses on indicating the different behaviour of sub-rectangular tunnels under  
14 static loading in comparison with circular and rectangular ones having the same uti-  
15 lization space. It allows designers to decide the appropriate tunnel shape solution  
16 that should be used. The influence of parameters, including soil deformability, lat-  
17 eral earth pressure coefficient, and lining thickness, on the behaviour of different  
18 tunnel shapes under static loadings is also investigated. The results indicated a sig-  
19 nificant difference in the behaviour of sub-rectangular tunnels in comparison with  
20 the circular and rectangular ones when considering no-slip and full-slip conditions  
21 for the soil–lining interaction.

22 **Keywords** Sub-rectangular tunnel · Static load · Tunnel lining · Numerical analysis

AQ1  
AQ2

### A1 Highlights

- A2 - Behaviour of differently shaped tunnel linings subjected to static loading was highlighted;  
A3 - Sub-rectangular tunnels can be an effective solution replacing circular and rectangular tunnel.

AQ3

A4 ✉ Daniel Dias  
A5 [daniel.dias@3sr-grenoble.fr](mailto:daniel.dias@3sr-grenoble.fr)

A6 <sup>1</sup> Faculty of Civil Engineering, Hanoi University of Mining and Geology, Bắc Từ Liêm, Vietnam

A7 <sup>2</sup> Department of Underground and Mining Construction, Faculty of Civil Engineering, Hanoi  
A8 University of Mining and Geology, Bắc Từ Liêm, Vietnam

A9 <sup>3</sup> Laboratory 3SR, CNRS UMR 5521, Grenoble Alpes University, 38000 Grenoble, France

## 23 1 1. Introduction

24 The rapid development of urban infrastructures and rising population density is the cause  
25 of the serious shortage of urban land and therefore traffic congestion. In dense urban  
26 areas, one of the solutions is to develop underground works to solve these difficulties.

27 Urban traffic often requires the connection of different routes such as terres-  
28 trial roads and overhead roads and is connected to tunnel routes. Tunnels are usu-  
29 ally located at shallow depth. Optimization of the tunnel shape is important to  
30 increase the cross-section utilization as well as the tunnel stability. Until now,  
31 circular tunnels (for mechanized tunnelling) or U-shapes (for conventional tun-  
32 nelling) are usually designed due to their advantage in terms of lining stability  
33 and also for circular shapes due to the tunnelling boring machines (TBMs) tech-  
34 nology. Circular shape has, however, a low space utilization ratio. On the con-  
35 trary, square and rectangular tunnels allow a high capacity of using cross-section,  
36 but their main disadvantage is the stresses concentration at the tunnel corners  
37 (Nakamura et al. 2003). Recently, a special cross-section tunnel named sub-rec-  
38 tangular has been developed (Liu et al. 2018; Zhang et al. 2017; Konstantin and  
39 Mikhail 2017; Zhu et al. 2017; Zhang et al. 2019). Sub-rectangular tunnels solve  
40 the shortcomings of both the circular and rectangular tunnels while keeping the  
41 advantages of a high space utilization ratio and general stability.

42 The influence of tunnel shapes on the tunnel's stability was studied in the lit-  
43 erature (Abdellah et al. 2018; Vinod and Khabbaz 2019; Do et al. 2020). Abdellah  
44 et al. (Abdellah et al. 2018) studied the stability of differently shaped tunnels, i.e.  
45 circular, square, and horseshoe tunnels, located at shallow depth. Vinod and Khab-  
46 baz. (Vinod and Khabbaz 2019) studied the effect of the tunnel shape on lining inter-  
47 nal forces induced by twin circular tunnels and twin rectangular tunnels. Do et al.  
48 (Do et al. 2020) investigated the influence of the parameters on the lining internal  
49 forces of squared or sub-rectangular tunnels. The results obtained by these researches  
50 illustrated a significant effect of the tunnel shape on tunnel lining behaviour. Unfortu-  
51 nately, the influence of circular, rectangular, and sub-rectangular tunnels on internal  
52 lining forces induced has not been yet thoroughly and simultaneously evaluated.

53 In this study, a numerical analysis is conducted to investigate the behaviour of sub-  
54 rectangular tunnels under static loading compared with circular and rectangular ones  
55 having the same utilization space. It allows designers to decide the appropriate tunnel  
56 shape solution that should be used. The effects of Young's modulus,  $E_s$ , the lateral  
57 earth pressure coefficient,  $K_0$ , and the lining thickness,  $t$ , are highlighted.

## 58 2 2. Numerical Simulations of Tunnels under Static Loading

### 59 2.1 Reference Sub-Rectangular Tunnel Case—Shanghai Tunnel Metro

60 The parameters of the sub-rectangular tunnel cross-section in this study were  
61 adopted from a constructed tunnel in Shanghai, China (Do et al. 2020). The

**Fig. 1.** Sub-rectangular express tunnel in Shanghai (Do et al. 2020), Distances in millimetres

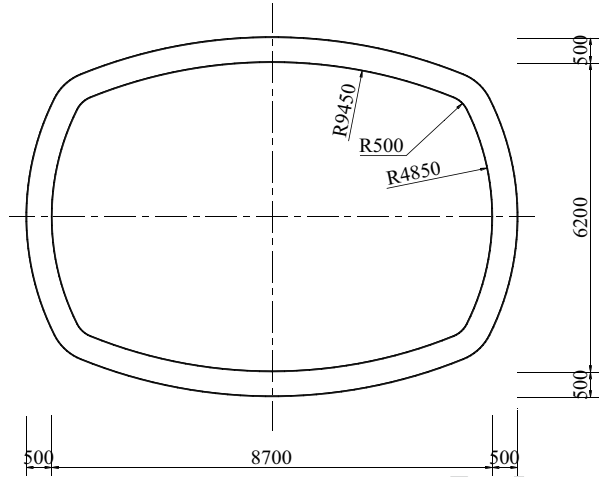
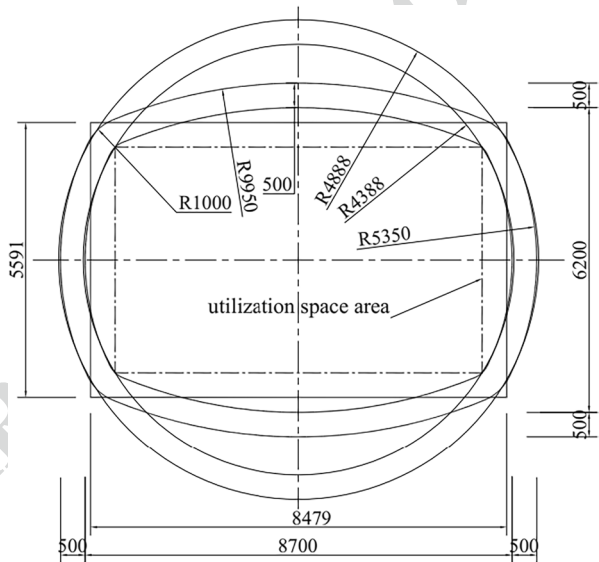


**Fig. 2.** Circular and Rectangular Tunnel with the Same Utilization Space Area, Distances in Millimetres



62 dimensions of the sub-rectangular tunnel are 9.7m in width and 7.2m in height  
 63 and an excavation area of 60 m<sup>2</sup> as shown in Fig. 1. The tunnel is supported by  
 64 segmental concrete linings of 0.5m in thickness. In this study, a continuous lining  
 65 was adopted without considering the joint effect. Based on this sub-rectangular  
 66 tunnel cross-section, a circular tunnel with a radius of 4.89m and a rectangular  
 67 tunnel with dimensions of 8.48m in width and 5.59m in height are built. They  
 68 have the same utilization space area as the sub-rectangular tunnel. The cross-section  
 69 excavation areas of the circular and rectangular tunnels are 75m<sup>2</sup> and 47m<sup>2</sup>,  
 70 respectively (Fig. 2).

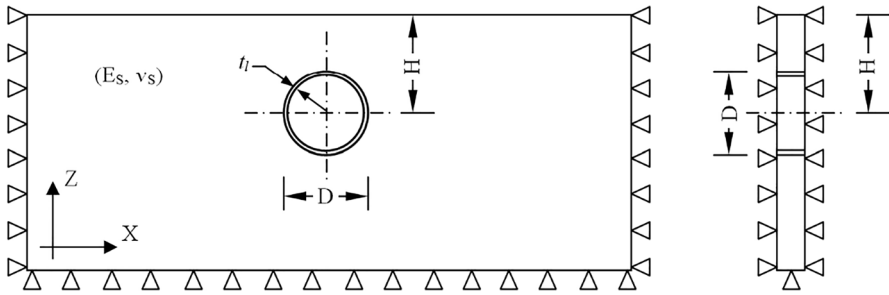


Fig. 3. Plane Strain Model under Consideration

Table 1. Input parameters of the soil and tunnel lining for the reference case

Parameter	Symbol	Unit	Value
Soil properties			
Unit weight	$\gamma$	kN/m <sup>3</sup>	18
Young's modulus	$E_s$	MPa	100
Poisson's ratio	$\nu_s$	-	0.34
Internal friction angle	$\phi$	degrees	33
Cohesion	$c$	kPa	0
Lateral earth pressure coefficient	$K_0$	-	0.5
Depth of tunnel	$H$	m	20
Tunnel lining properties			
Young's modulus	$E_l$	GPa	35
Poisson's ratio	$\nu_l$	-	0.15
Lining thickness	$t$	m	0.5
External diameter of circular tunnel	$D$	m	9.76
Dimensions of the sub-rectangular tunnel	W x H	m	9.7 x 7.2
Dimensions of the rectangular tunnel	W x H	m	8.48 x 5.95

71 **2.2 Tunnels Numerical Model**

72 2D numerical models of different tunnel shapes, i.e. circular, rectangular, and sub-rec-  
 73 tangular ones, are simulated. Figure 3 shows a typical 2D numerical model in plane  
 74 strain conditions in the case of a circular tunnel. These models were considered to  
 75 quantify the behaviour of tunnel linings under static loading. It is assumed that the tun-  
 76 nel structure's behaviour and soil mass are linear elastic. The properties of soil and dif-  
 77 ferent tunnel lining shapes are given in Table 1.

78 In this study, numerical simulations are performed employing the Flac<sup>3D</sup> finite dif-  
 79 ference program (Itasca Consulting Group,FLAC Fast Lagrangian Analysis of Con-  
 80 tinua, 2012,Version 5.0. User's manual, Available: <http.itascacg.com> 2012). Hexa-  
 81 hedral zones are used for discretizing the volume under study. The tunnel linings are  
 82 modelled using embedded liner elements. Embedded liner elements are linked to the

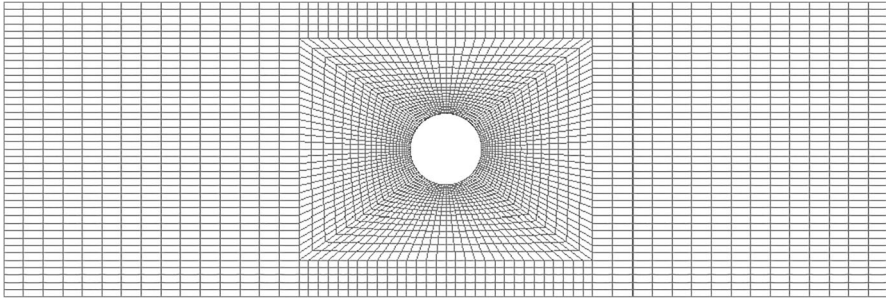


Fig. 4. Geometry and Mesh for the Circular Tunnel Model

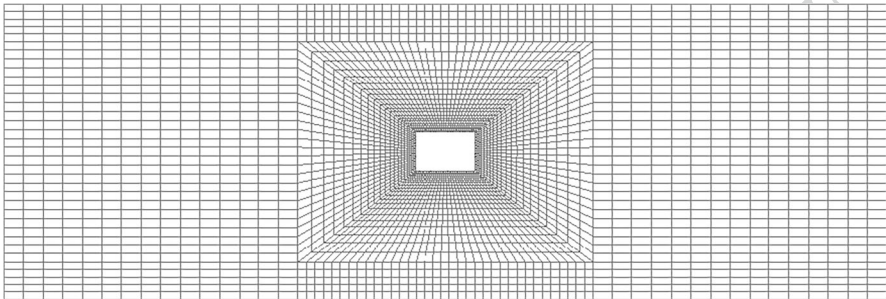


Fig. 5. Geometry and Mesh for the Rectangular Tunnel Model

83 zone faces along the tunnel boundary through interface stiffness (normal stiffness  $k_n$   
 84 and tangential stiffness  $k_s$ ). The values of  $k_n$  and  $k_s$  are set to one hundred times the  
 85 equivalent stiffness of the stiffest neighbouring zone (Itasca Consulting Group,FLAC  
 86 Fast Lagrangian Analysis of Continua, 2012,Version 5.0. User's manual, Available:  
 87  $\langle$ http.itascacg.com $\rangle$  2012) for the no-slip condition case. When considering the full-  
 88 slip condition,  $k_s$  is assigned to be equal to zero. The apparent stiffness (expressed in  
 89 stress-per-distance units) of a mesh zone in the direction normal to the surface can be  
 90 calculated by using the following formula:

91

$$\mathbf{max} \left[ \frac{\left( K + \frac{4}{3}G \right)}{\Delta z_{\min}} \right] \quad (1)$$

92  
 93 where  $K$  and  $G$  are the bulk and shear modulus, respectively.  
 94  $\Delta z_{\min}$  is the smallest dimension in the normal zones direction that enters in con-  
 95 tact with the liner elements.

96 The mesh consisted of a single layer of zones in the  $y$ -direction, and the size of  
 97 the elements increases as one moves away from the tunnel (Figs. 4, 5, and 6 cor-  
 98 responding to, respectively, the circular, rectangular, and sub-rectangular tunnels).  
 99 The numerical model is 120 m wide in the  $x$ -direction. The two vertical boundaries

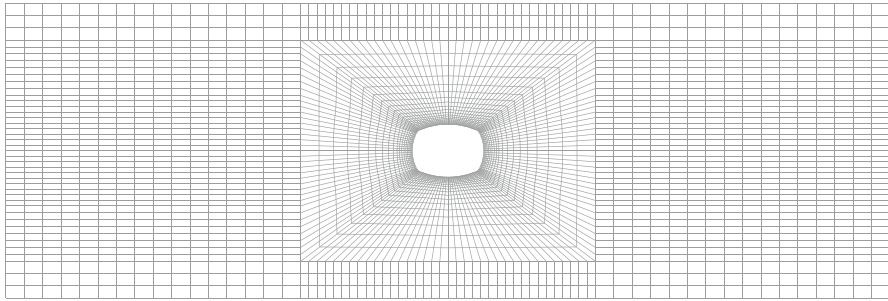


Fig. 6. Geometry and Mesh for the Sub-rectangular Tunnel Model

100 are fixed in the horizontal direction. (40 m high in the z-direction). The surface of the  
 101 model is free, and the bottom was blocked in all directions. It consists of approx-  
 102 imately 4,800 zones and 9,802 nodes for the circular tunnel, 4,675 zones, and 9,552  
 103 nodes for the rectangular tunnel, and the sub-rectangular is 5,816 zones and 11,870  
 104 nodes.

105 The first step of the numerical excavation process is to set up the model and assign  
 106 the plane strain boundary conditions and the initial stress state taking into considera-  
 107 tion the gravity field. Then, the tunnel is excavated and the lining is assigned in the  
 108 second step. Relaxation of the ground between the excavation boundary and the lin-  
 109 ing setup was not considered. This case corresponds to the worst one for the lining  
 110 stress state.

### 111 2.3 Comparison of Different Shaped Tunnel Linings under Static Loading

112 Figure 7a illustrates the bending moments in the tunnel lining for the three types of  
 113 tunnels: circular, rectangular, and sub-rectangular. Firstly, in comparison with the  
 114 rectangular and sub-rectangular tunnel, the bending moments in the circular tun-  
 115 nel are the smallest for both the no-slip and full-slip cases. The extreme bending

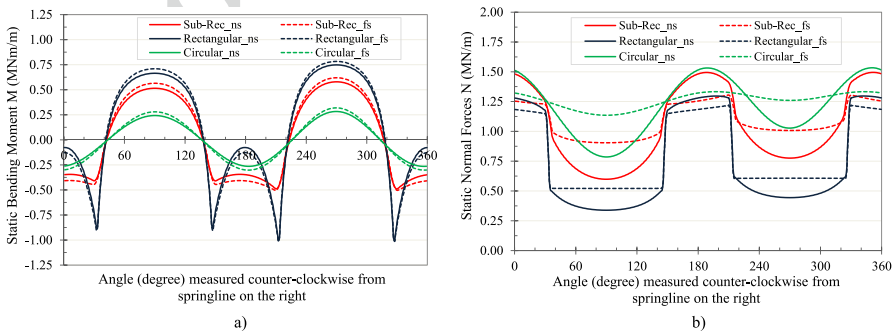


Fig. 7. Internal Forces Induced in Circular, Sub-rectangular, and Rectangular Tunnels a) Bending Moment b) Normal Forces **AQ4**



116 moments are observed at the crown, bottom and two sides of the tunnel. In the rec-  
117 tangular tunnel, while the smallest bending moments are obtained in the corners of  
118 the rectangular tunnel, the maximum positive bending moments are observed at the  
119 tunnel crown and bottom. As for the sub-rectangular tunnel, the bending moment  
120 values are in between those obtained in the two other tunnel cross-sections. The  
121 bending moments are not concentrated at the four corners as can be seen for the  
122 rectangular tunnel. The bending moments distribution in the tunnel linings is con-  
123 cerned by the fact that corners or sharp positions with small radius cause stress con-  
124 centrations and prevent the forces redistribution along the tunnel boundaries. The  
125 tunnel boundaries should therefore be designed as much curves as possible.

126 Considering the lining–soil interaction influence, the bending moments in the  
127 full-slip case are slightly larger than the ones in the no-slip case. The discrepancy  
128 of the maximum bending moments induced in circular, sub-rectangular, and rectan-  
129 gular tunnels considering the two cases of no-slip and full-slip conditions is 13%, 7  
130 %, and 5%, respectively. Those of the minimum bending moments in circular and  
131 sub-rectangular tunnels are 14% and 3%. However, there is almost no difference for  
132 the minimum bending moments between no-slip and full-slip conditions for rectan-  
133 gular tunnels. The lining–soil interaction influence on the tunnel lining’s bending  
134 moments is of main importance for circular tunnels. It decreases for sub-rectangular  
135 and rectangular tunnels. Circumferential movements of circular tunnel linings do not  
136 present corners and sharp positions as they can be seen in rectangular and sub-rec-  
137 tangular tunnels, respectively.

138 As shown in Fig. 7b, while the smallest minimum normal forces are observed  
139 for rectangular tunnels, the largest maximum normal forces are obtained for the cir-  
140 cular tunnel, for both no-slip and full-slip conditions. The minimum normal forces  
141 for the rectangular tunnel are significantly smaller than those of the two other tun-  
142 nels shapes (circular and sub-rectangular). This could be explained by the lower  
143 transmission effect of the lateral loading from the two tunnel sides to the crown and  
144 bottom parts in the case of a rectangular tunnel. It should be mentioned that for  
145 small normal forces induced in the tunnel lining, the maximum allowable bending  
146 moments will be reduced. That is why small normal forces can be considered as  
147 unfavourable for structure stability.

148 Figure 7b shows a great influence of soil–lining interaction, i.e. full-slip and  
149 no-slip conditions, on the normal forces developed in the tunnel lining. The most  
150 important change is observed at the crown and bottom area of tunnels. For all  
151 three tunnel shapes, while maximum normal forces are seen at the sidewall, mini-  
152 mum values are observed at the top or bottom. It could be related to the low lat-  
153 eral earth pressure factor,  $K_0$ , used in this study. It causes greater vertical loadings  
154 principally transiting into structures at the sidewalls. For higher  $K_0$  values, the  
155 loading will mainly transfer to the tunnel top and bottom. In general, the maxi-  
156 mum normal forces obtained at the tunnel sidewalls in the full-slip condition  
157 are significantly smaller than for the no-slip condition. However, the minimum  
158 normal forces observed at the tunnel’s top and bottom in the full-slip condition  
159 are greater than the ones in the no-slip case, 45%, 51%, and 54% with the circu-  
160 lar tunnel, sub-rectangular, and rectangular tunnel, respectively. The lining–soil  
161 interaction influence on the lining normal forces could be explained by the tight

162 connection in the no-slip condition. It helps to better distribute the ground load-  
 163 ing between tunnel parts, i.e. from the top and bottom to the sidewalls and vice  
 164 versa. This load redistribution is less effective for the full-slip condition. It causes  
 165 smaller differences between maximum normal forces at the tunnel's top and  
 166 minimum one at the sidewalls in the full-slip condition case compared with the  
 167 no-slip one as indicated in Fig. 7b. It is also interesting to note that the internal  
 168 forces in the sub-rectangular tunnel are in between the circular and rectangular  
 169 tunnels ones.

170 Based on the combined evaluation of the bending moments and normal forces  
 171 induced in the tunnel lining of the three above shapes, the rectangular tunnel is  
 172 the worst case in terms of stability and the circular tunnel is the most stable one.  
 173 In addition, the tunnel will be more efficiently supported in no-slip conditions  
 174 compared to the full-slip ones.

175 Normal displacements induced in circular, sub-rectangular, and rectangular  
 176 tunnels are introduced in Fig. 8. While the smallest displacement is observed in  
 177 circular tunnels, the largest ones occurred in rectangular tunnels. Due to the low  
 178 lateral earth pressure factor,  $K_0$  of 0.5, maximum displacements are seen at the  
 179 top and bottom of the tunnel for both no-slip and full-slip cases. It should be also  
 180 noted that the full-slip interaction between the soil and tunnel lining is followed  
 181 by a slightly greater displacement. It is in good agreement with the larger bending  
 182 moment in full-slip conditions as indicated in Fig. 7a.

### 183 3 Parametric Study

184 The results in Figs. 7 and 8 give a clear understanding of the behaviour of circu-  
 185 lar, rectangular, and sub-rectangular tunnel linings considering both no-slip and  
 186 full-slip conditions. In the next sections, a parametric study is conducted to high-  
 187 light the behaviour of sub-rectangular tunnels compared with circular and rectangu-  
 188 lar ones. The effect of parameters, like the lateral pressure coefficient,  $K_0$ , Young's

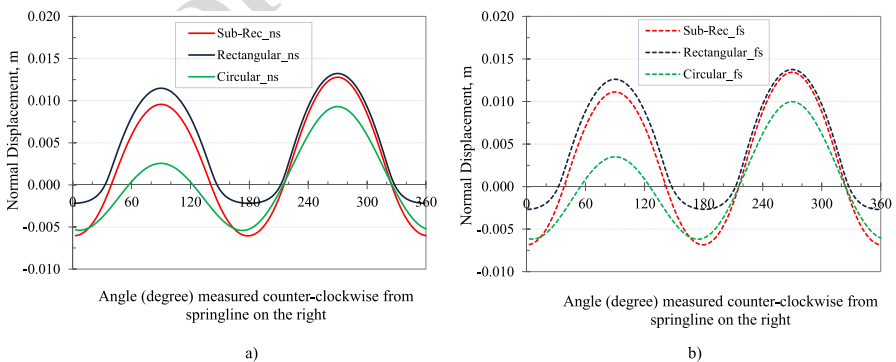


**Fig. 8.** Normal Displacements Induced in Circular, Sub-rectangular, and Rectangular Tunnels **a)** Normal displacement in no-slip case **b)** Normal displacement in full-slip case

189 modulus,  $E_S$ , and lining thickness,  $t$ , considering the soil–lining interface conditions  
 190 is investigated.

191 **3.1 Effect of the Young's Modulus,  $E_S$**

192 The Young's modulus values are assumed to vary in a wide range from 25 to 350  
 193 MPa. The other parameters based on the reference case are considered (Table 1).  
 194 Results of internal forces in circular, rectangular, and sub-rectangular tunnel linings  
 195 for both no-slip and full-slip conditions are shown in Fig. 9.

196 Figure 9a and b shows that when  $E_S$  value increases from 25 to 50 MPa, the abso-  
 197 lute extreme bending moments decrease sharply. When the  $E_S$  value is larger than 50  
 198 MPa, an increase in the  $E_S$  value causes a slight reduction in the absolute extreme  
 199 bending moments. This variable trend is seen in all three cross-sections of tunnel  
 200 linings. The extreme bending moments in the full-slip condition are always greater  
 201 than the ones in the no-slip condition. It should be noted that the minimum bending

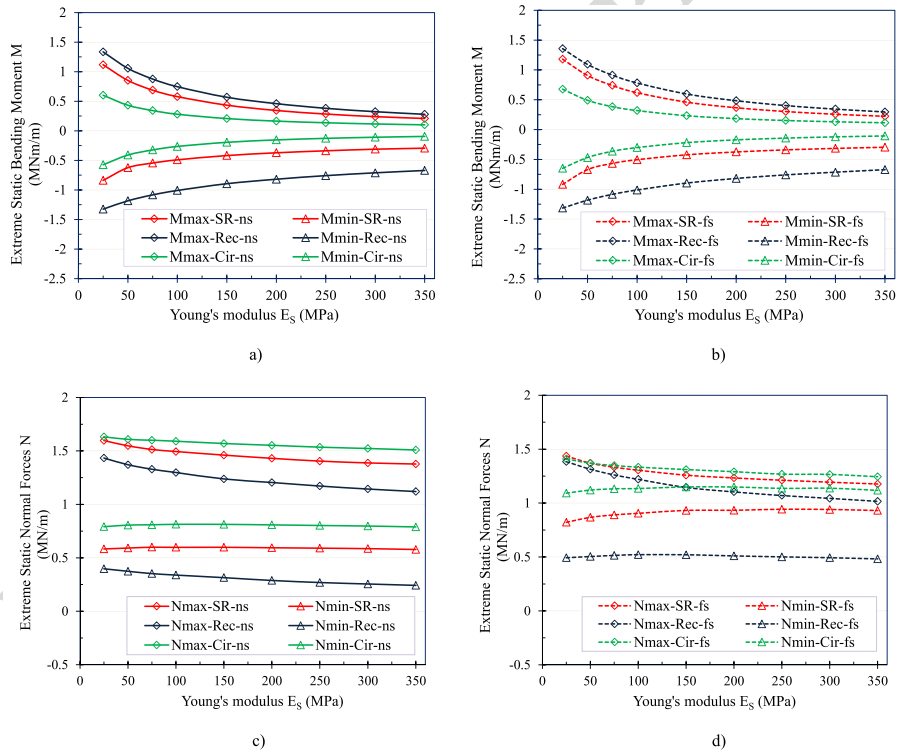


**Fig. 9.** Effect of Young's Modulus on the Internal Forces in the Tunnel Linings **a)** Extreme bending moments in no-slip case **b)** Extreme bending moments in full-slip case **c)** Extreme normal forces in no-slip case **d)** Extreme normal forces in full-slip case

202 moments in the rectangular tunnel are smaller than the ones in circular and sub-  
 203 rectangular tunnels and both for the no-slip and full-slip conditions.

204 For the no-slip condition, Fig. 9c indicates a slight decrease in the maximum normal  
 205 normal forces (<10%). The minimum normal forces in both sub-rectangular and circular  
 206 tunnels stayed more less constant when the  $E_S$  value increases, while the absolute  
 207 extreme normal forces in rectangular tunnels tend to decrease gradually (25%). Fig-  
 208 9d shows that the maximum normal tunnel lining forces in full-slip condition  
 209 are smaller than the ones in no-slip condition when the  $E_S$  increases from 25 to 350  
 210 MPa. It should be noted that the extreme normal forces in the rectangular tunnel  
 211 are strongly affected by the  $E_S$  value compared to the sub-rectangular and circular  
 212 tunnels (steeper lines in Fig. 9d). The dependency of the normal forces in the sub-  
 213 rectangular and circular tunnels on the  $E_S$  value is more or less similar.

214 Figure 10 introduces the dependency of the normal displacements on the  $E_S$   
 215 value. The variation in the maximum inward displacements induced at the bottom  
 216 of rectangular and sub-rectangular tunnels is nearly similar and greater than in cir-  
 217 cular tunnels. Meanwhile, outward displacements occurred at the sidewalls of the  
 218 circular and sub-rectangular tunnels are relatively the same and larger than the rec-  
 219 tangular tunnel ones (Fig. 10a, b). This could be concerned with the curve radius  
 220 effect in circular and sub-rectangular tunnels compared with the straight lining parts  
 221 of rectangular tunnels. Indeed, the curved lining is more efficient in preventing the  
 222 inward displacements at the top and bottom of the tunnel. On the other hand, straight  
 223 lining parts and corners in rectangular tunnels cause a smaller forces redistribution  
 224 from the top and bottom to the sidewall. It, therefore, induces smaller bending forces  
 225 developed in the lining at the sidewalls. As a consequence, outward displacements in  
 226 rectangular tunnels are small as indicated in Fig. 10b.

227 **3.2 Effect of the lateral earth pressure,  $K_0$**

228 Lateral earth pressure values are assumed to vary in a range from 0.3 to 2.0 while  
 229 the other parameters of the reference case in Table 1 are used. The results pre-  
 230 sented in Fig. 11 indicate that the  $K_0$  has a great effect on the internal forces of

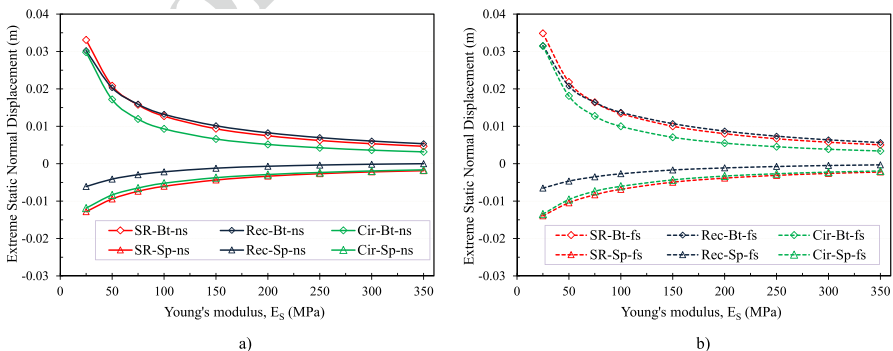


**Fig. 10.** Effect of Young's Modulus on the Normal Displacement in the Tunnel Linings a) Extreme static normal displacement for no-slip case b) Extreme static normal displacement for full-slip case

Transportation Infrastructure Geotechnology

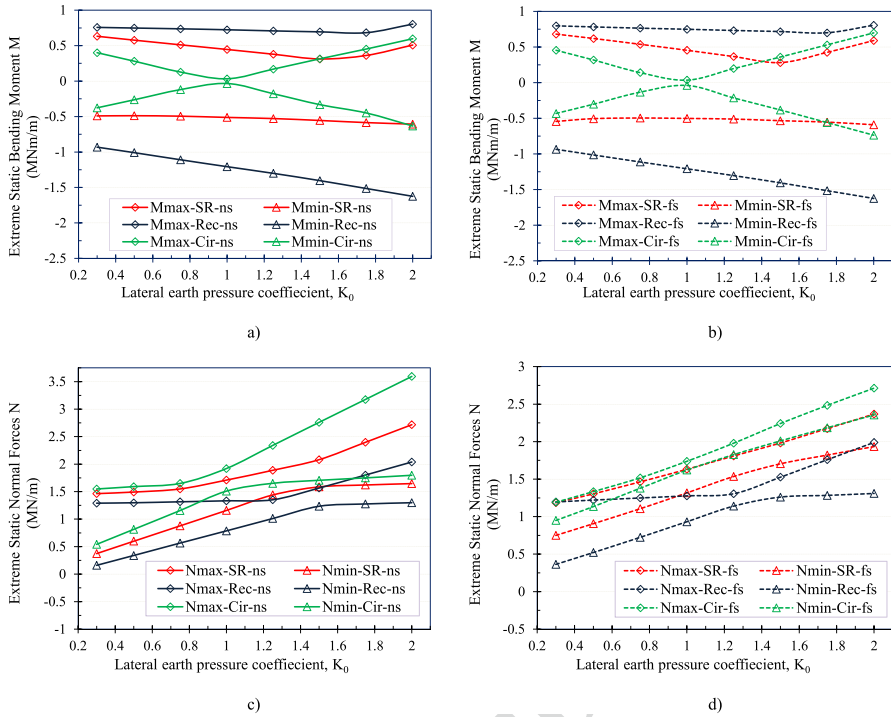


**Fig. 11.** Effect of the Lateral Earth Pressure Coefficient on the Internal Forces in the Tunnel Linings **a)** Extreme bending moment for no-slip case **b)** Extreme bending moment for full-slip case **c)** Extreme normal forces for no-slip case **d)** Extreme normal forces for full-slip case

231 the three tunnels and in both no-slip and full-slip conditions. It is also noted that  
 232 there is a great influence of the tunnel shapes on the tunnel lining’s internal forces  
 233 induced when the  $K_0$  values change.

234 Figure 11a, b illustrates that the absolute extreme bending moments in the circular  
 235 tunnel greatly change depending on the  $K_0$  values. They reach the minimum  
 236 values when the  $K_0$  value is equal to the unity. When the  $K_0$  value is smaller than  
 237 unity, positive bending moments are observed at the top and bottom of the tunnel.  
 238 When  $K_0$  value increases, positive bending moments occurred at the sidewalls.  
 239 In other words, positive bending moments appeared at lining parts being perpen-  
 240 dicular with the maximum stress direction (Fig. 11a, b).

241 Different from the circular tunnel, these figures show a slight influence of the  
 242  $K_0$  value on the maximum bending moments for the rectangular tunnels. How-  
 243 ever, the absolute value of the minimum bending moments in the rectangular tun-  
 244 nels increases linearly when the  $K_0$  value increases from 0.3 to 2.0. It is one of the  
 245 main drawbacks of rectangular tunnels. The lower influence of the  $K_0$  value on  
 246 the bending moments in rectangular tunnels is related to the small redistribution  
 247 effect of the lining forces from the sidewall to the top and bottom parts as men-  
 248 tioned in section 2.3. Consequently, greater horizontal forces from the sidewall

249 caused by the increase in  $K_0$  value cause insignificant forces changes preventing  
 250 again inward vertical movements at the top and bottom parts of the tunnel lining.

251 Sub-rectangular tunnels seem to overcome this drawback. Indeed, the minimum  
 252 bending moments at the 4 shoulders are almost constant when  $K_0$  increases from  
 253 0.3 to 2.0 for both full-slip and no-slip conditions. The maximum bending moments  
 254 induced in sub-rectangular tunnels tend to decrease and reach the minimum value at  
 255  $K_0$  values of approximately 1.6.

256 Considering the interaction between the lining and soil, the absolute extreme  
 257 bending moments in the circular tunnels in the full-slip condition are 15% greater  
 258 than the ones in the no-slip condition (Fig. 11a, b). For the rectangular tunnels, there  
 259 is no clear difference in the minimum extreme bending moments at the four tunnel  
 260 lining corners between the full-slip and no-slip conditions. It is due to the rectangu-  
 261 lar tunnel corners which decrease the soil–lining interaction effect on the internal  
 262 forces.

263 Particular attention should then be paid to sub-rectangular tunnels; the maximum  
 264 bending moments in the full-slip conditions are lower than the ones in the no-slip  
 265 condition when the  $K_0$  value changes from 1.25 to 1.5. It is similar; at the 4 shoul-  
 266 ders, the absolute minimum bending moments in the no-slip condition are higher  
 267 than the ones in the full-slip condition, corresponding to  $K_0$  values from 1 to 2.

268 Figure 11c and d indicates that the extreme normal forces in the tunnel linings  
 269 increase in all the tunnel shape cases when the  $K_0$  increases. The maximum and  
 270 minimum normal forces in circular tunnels are always greater than the correspond-  
 271 ing sub-rectangular and rectangular ones

272 Figure 12 indicates that a  $K_0$  value increase causes a decrease in the inward  
 273 displacements at the top and bottom of the tunnel. It is then followed by outward  
 274 displacements for larger  $K_0$  values. Meanwhile, outward displacements induced at the  
 275 sidewalls observed at low  $K_0$  values are modified to inward displacements for large  
 276  $K_0$  values. The extreme displacements variation in rectangular tunnels depending on  
 277 the  $K_0$  values is lower than those on sub-rectangular and circular tunnels.

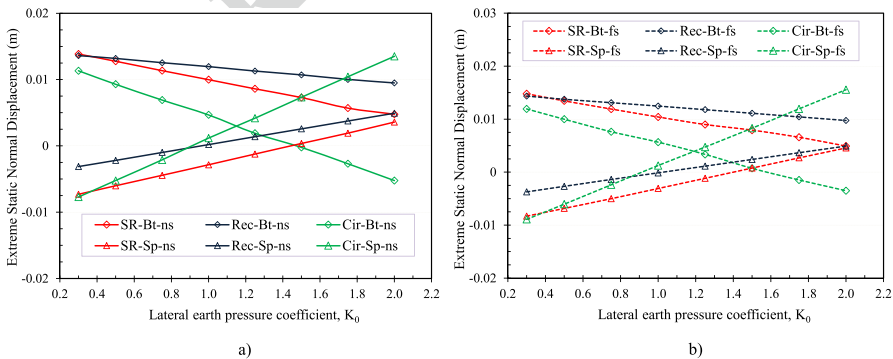


**Fig. 12.** Effect of the Lateral Earth Pressure Coefficient on the Normal Displacement in the Tunnel Linings **a)** Extreme static normal displacement for no-slip case **b)** Extreme static normal displacement for full-slip case

278 **3.3 Effect of the Lining Thickness**

279 The lining thickness  $t$  is assumed to vary in the range from 0.2 to 0.8 m, and the  
 280 other parameters are taken as shown in Table 1. The results presented in Fig. 13  
 281 indicate that the  $t$  value has a great effect on the extreme internal forces for all cases  
 282 of tunnel shapes for both no-slip and full-slip conditions. The relationship between  
 283 the absolute extreme internal forces and the lining thickness for the considered cases  
 284 is quite linear.

285 Figure 13a, b shows that the absolute extreme bending moments in circular tunnel  
 286 linings are always the smallest and in rectangular tunnels are the biggest when  
 287 the lining thickness increases from 0.2 to 0.8 m. The absolute extreme bending  
 288 moments in the full-slip condition are larger than the ones in the no-slip condition  
 289 as indicated in section 2.3. The greatest and smallest dependency of the maximum  
 290 bending moments on the lining thickness is, respectively, observed in rectangular  
 291 and circular tunnels. It means that rectangular tunnels are more sensitive to the lin-  
 292 ing thickness change in terms of the bending moments.

293 As for the extreme normal forces in the circular and sub-rectangular tunnels,  
 294 they vary less in no-slip conditions. Generally, slight increases in the maximum

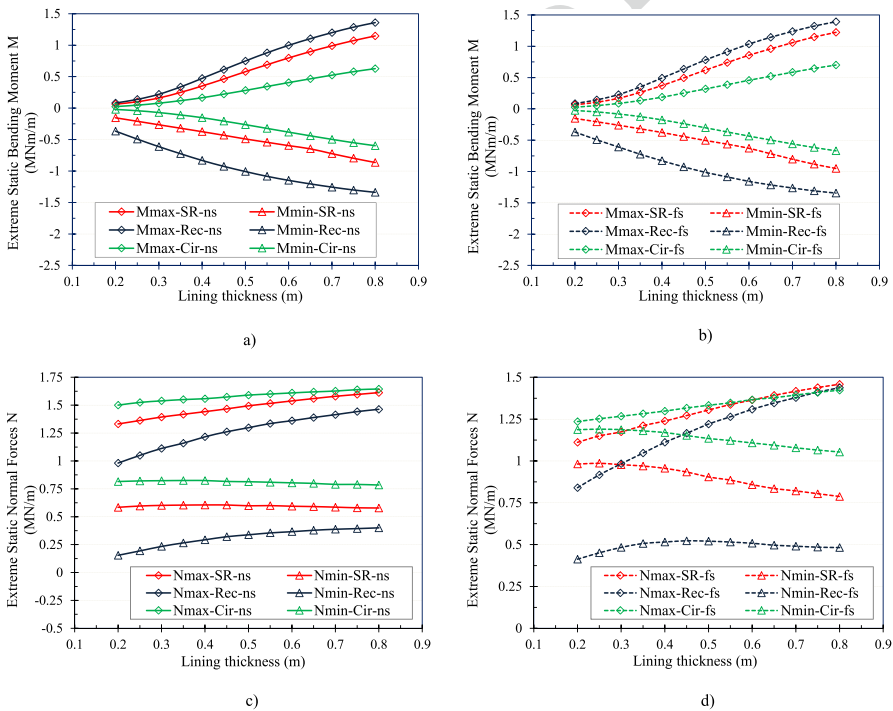


**Fig. 13.** Effect of the Lining Thickness on the Tunnel Lining Internal Forces a) Extreme bending moment for no-slip case b) Extreme bending moment for full-slip case c) Extreme normal forces for no-slip case d) Extreme normal forces for full-slip case

295 normal forces are observed when the lining thickness increases from 0.2 to 0.8m.  
 296 In contrast, a greater variation in the normal forces is seen for rectangular tunnels  
 297 (Fig. 13c). In the full-slip case, an increase in the lining thickness causes a slight  
 298 decrease in the minimum normal forces and an increase in the maximum normal  
 299 forces for all three tunnel shapes (Fig. 13d). It should be noted that smaller maxi-  
 300 mum normal forces in the three kinds of tunnels are observed when the lining is  
 301 thicker (Fig. 13c, d). In other words, thicker linings will decrease the tunnel shape  
 302 effect on the maximum normal forces.

303 Figure 14 presents extreme normal displacements with the lining thickness varia-  
 304 tion. The biggest and smallest dependency occurred in rectangular and circular tun-  
 305 nels, respectively. Displacements in the tunnel lining decrease when the lining thick-  
 306 ness increases. Similar to the normal forces, the thicker lining causes a lower tunnel  
 307 shape influence on the lining displacements.

#### 308 4 4. Conclusions

309 A 2D numerical parametric study is conducted to highlight the behaviour of circu-  
 310 lar, rectangular, and sub-rectangular tunnels under static loading. Parameters, like  
 311 Young's modulus, lateral earth pressure, lining thickness, were investigated. Based  
 312 on the research results, there are some conclusions as follows:

313 - In terms of space utilization ratio efficiency, the circular tunnel gives the worst  
 314 performance compared to the two other cross-sections. By contrast, there is not  
 315 much difference in the space utilization ratio when comparing the sub-rectangular  
 316 and rectangular tunnels,

317 - Investigating the  $E_S$ ,  $K_0$ , and  $t$  parameters effect on the tunnel lining shows that  
 318 the circular tunnel is the most stable tunnel shape and the rectangular tunnel is the  
 319 worst shape in terms of stability. The high-stress concentration at the four corners  
 320 of the rectangular tunnel can be minimized when using the sub-rectangular tunnel,  
 321 and its stability is relatively good when compared to the circular tunnel. It should be

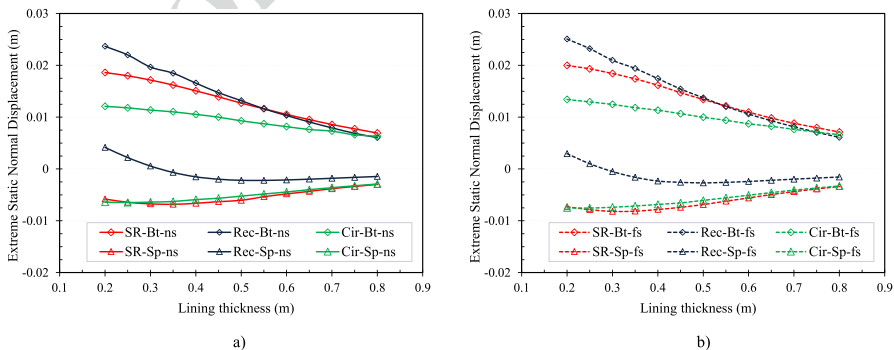


**Fig. 14.** Effect of the Lining Thickness on the Normal Displacement in Tunnel Lining **a)** Extreme static normal displacement for no-slip case **b)** Extreme static normal displacement for full-slip case



322 noted that the sub-rectangular is more efficient when the lateral earth pressure coefficient  
323 gradually increases, specifically for  $K_0 > 1.5$ . The maximum bending moments  
324 in the sub-rectangular tunnels are even smaller than the circular tunnel ones with the  
325 same utilization space area. In addition, the tunnel will be more efficiently supported  
326 in no-slip conditions compared to the full-slip ones.

327 Based on the obtained results, it is reasonable to conclude that sub-rectangular  
328 shaped tunnels should be considered as a potential solution to replace circular and  
329 rectangular tunnels due to their high utilization space ratio, and especially good stability  
330 by avoiding the stress concentration at the four corners.

331 **Acknowledgements** This research is supported by Ministry of Education and Training (Vietnam).

332 **Author's Contributions** Study conception and design were performed by Ngoc Anh Do and Daniel Dias.  
333 Material preparation and data collection were performed by Van Vi Pham, Chi Thanh Nguyen, Van Kien  
334 Dang. Data analyses were performed by Van Vi Pham, Ngoc Anh DO, Daniel Dias. The first draft of the  
335 manuscript was written by Van Vi Pham, and all authors commented on previous versions of the manu-  
336 script. All authors read and approved the final manuscript.

337 **Funding** This research is supported by the Vietnam Ministry of Education and Training.

338 **Data Availability** The datasets generated during and/or analysed during the current study are available  
339 from the corresponding author on reasonable request.

## 340 **Declarations**

341 **Ethics Approval and Consent to Participate** Not applicable

342 **Consent for Publication** Not applicable

343 **Competing Interests** The authors have no competing interests to declare that are relevant to the content  
344 of this article.

## 345 **References**

- 346 Nakamura, H., Kubota, T., Furukawa, M.: Unified construction of running track tunnel and crossover  
347 tunnel for subway by rectangular shape double track crosssection shield machine. *Tunnel. Undergr.*  
348 *Space Technol.* **18**(2), 253–62 (2003)
- 349 Liu, X., Ye, Y., Liu, Z., Huang, D.: Mechanical behavior of Quasi-rectangular segmental tunnel linings:  
350 first results from full-scale ring tests. *Tunn. Undergr. Space Technol.* **71**, 440–53 (2018)
- 351 Zhang, Z.X., Zhu, Y.T., Zhu, Y.F.: Development and application of a 1:1 mechanical test system for spe-  
352 cial-shaped shield lining with a large cross-section. *Chin. J. Rock Mech. Eng.* **12**(36), 2895–905  
353 (2017). ((in Chinese))
- 354 Konstantin, P.B., Mikhail, O.L.: About rock pressure loads on tunnel linings constructed using trenchless  
355 method. *J. Min. Instit.* **228**, 649–53 (2017)
- 356 Zhu, Y.T., Zhang, Z.X., Zhu, Y.F., Huang, X., Zhuang, Q.: Capturing the cracking characteristics of con-  
357 crete lining during prototype tests of a special-shaped tunnel using 3D DIC photogrammetry. *Eur. J.*  
358 *Environ. Civ. Eng.* **22**, 1–21 (2017)
- 359 Zhang, Z., Zhu, Y., Huang, X., Zhu, Y., Liu, W.: Standing full-scale loading tests on the mechanical  
360 behavior of a special-shape shield lining under shallowly-buried conditions. *Tunn. Undergr. Space*  
361 *Technol.* **86**(1), 34–50 (2019)

- 362 Abdellah, W.R., Ali, M.A., Yang, H.S.: Studying the effect of some parameters on the stability of shallow  
363 tunnels. *J. Sustain. Min.* **17**(1), 20–33 (2018)
- 364 Vinod, M., Khabbaz, H.: Comparison of rectangular and circular bored twin tunnels in weak ground.  
365 *Undergr. Space* (2019). <https://doi.org/10.1016/j.undsp.2019.03.004>
- 366 Do, N.A., Dias, D., Zixin, Z., Xin, H., Nguyen, T.T., Pham, V.V., Ouahcène, N.R.: Study on the behavior  
367 of squared and sub-rectangular tunnels using the Hyperstatic Reaction Method. *Transp. Geotech.*  
368 **22**, 100321 (2020)
- 369 Itasca Consulting Group, *FLAC Fast Lagrangian Analysis of Continua*, 2012, Version 5.0. User's manual,  
370 Available: (<http://itascacg.com>).

371 **Publisher's Note** Springer Nature remains neutral with regard to jurisdictional claims in published  
372 maps and institutional affiliations.  
373

UNCORRECTED PROOF

Journal:	<b>40515</b>
Article:	<b>230</b>

## Author Query Form

**Please ensure you fill out your response to the queries raised below  
and return this form along with your corrections**

Dear Author

During the process of typesetting your article, the following queries have arisen. Please check your typeset proof carefully against the queries listed below and mark the necessary changes either directly on the proof/online grid or in the 'Author's response' area provided below

Query	Details Required	A u t h o r ' s Response
<a href="#">AQ1</a>	City in affiliation 1 and 2 has been provided. Please check if correct.	
<a href="#">AQ2</a>	Please check if affiliations are presented correctly.	
<a href="#">AQ3</a>	Please check captured article note "Highlights:" if correct.	
<a href="#">AQ4</a>	Please check Figure captions with panels if correct.	